

## Research paper

# Lipid nanoparticles for alkyl lysophospholipid edelfosine encapsulation: Development and *in vitro* characterization

Ander Estella-Hermoso de Mendoza <sup>a</sup>, Marta Rayo <sup>a</sup>, Faustino Mollinedo <sup>b</sup>,  
María J. Blanco-Prieto <sup>a,\*</sup>

<sup>a</sup> Department of Pharmacy and Pharmaceutical Technology, University of Navarra, Pamplona, Spain

<sup>b</sup> Instituto de Biología Molecular y Celular del Cáncer, CSIC-Universidad de Salamanca, Salamanca, Spain

Received 15 March 2007; accepted in revised form 18 June 2007

Available online 30 June 2007

---

## Abstract

The ether lipid 1-*O*-octadecyl-2-*O*-methyl-*rac*-glycero-3-phosphocholine, edelfosine (ET-18-OCH<sub>3</sub>) is the prototype molecule of a promising class of antitumor drugs named alkyl-lysophospholipid analogues (ALPs) or antitumor ether lipids. This drug presents a very important drawback as can be the dose dependent haemolysis when administered intravenously. Lipid nanoparticles have been lately proposed for different drug encapsulation as an alternative to other controlled release delivery systems, such as liposomes or polymeric nanoparticles. The aim of this study was to develop a lipid nanoparticulate system that would decrease systemic toxicity as well as improve the therapeutic potential of the drug. Lipids employed were Compritol® 888 ATO and stearic acid. The nanoparticles were characterized by photon correlation spectroscopy for size and size distribution, and atomic force microscopy (AFM) was used for the determination of morphological properties. By both differential scanning calorimetry (DSC) and X-ray diffractometry, crystalline behaviour of lipids and drug was assessed. The drug encapsulation efficiency and the drug release kinetics under *in vitro* conditions were measured by HPLC-MS. It was concluded that Compritol® presents advantages as a matrix material for the manufacture of the nanoparticles and for the controlled release of edelfosine.

© 2007 Elsevier B.V. All rights reserved.

**Keywords:** Lipid nanoparticles; Edelfosine; Drug delivery; Atomic force microscopy; Differential scanning calorimetry; X-ray diffractometry

---

## 1. Introduction

Edelfosine (ET-18-OCH<sub>3</sub>, 1-*O*-octadecyl-2-*O*-methyl-*rac*-glycero-3-phosphocholine), is the prototype of a promising class of antitumor agents, collectively known as alkyl-lysophospholipid analogues (ALPs) or antitumor ether lipids, that do not target the DNA, but affect the cell membrane and the apoptotic machinery of the cancer cell [1]. Phase I studies have shown a good tolerability of the drug but with haematological and systemic side effects

[1,2]. However, although edelfosine has been shown to exert potent antineoplastic effects *in vitro* [3,4], the antitumor activity in phase II clinical studies has been only moderate [5]. Moreover, ALPs show manifold biological effects in addition to their antineoplastic actions, including an antiparasitic effect on *Leishmania* [6] as well as an inhibition of the cell membrane phospholipid turnover [7] and a potent inhibition of neovascularization [8], protein kinase C and Na<sup>+</sup>/K<sup>+</sup>-ATPase [9].

Edelfosine has also been given intravenously, but this provoked haemolysis as a major side effect [10]. This led to the only formulation developed so far, the TLC ELL-12, in which edelfosine was included into liposomes [11] to avoid the haemolytic toxicity of the drug. However, the main inconvenience of liposomes is their rapid clearance from plasma in comparison with other delivery systems.

---

\* Corresponding author. Department of Pharmacy and Pharmaceutical Technology, School of Pharmacy, University of Navarra, C/Irunlarrea 1, E-31080 Pamplona, Spain. Tel.: +34 948 425 600x6519; fax: +34 948 425 649.

E-mail address: [mjblanco@unav.es](mailto:mjblanco@unav.es) (M.J. Blanco-Prieto).

Lipid nanoparticles have been proposed as an alternative for the existing traditional particulate systems, such as previously mentioned liposomes or polymeric nanoparticles. These particulate systems made from solid lipids started being developed in the early 1990s. They provide physical stability, controlled release and a wide variety of application routes (parenteral, oral, dermal, ocular, pulmonary and rectal) [12–16].

Lipid nanoparticles are basically composed of a high melting point lipid that acts as a solid core, covered by surfactants. Lipids used to form these matrices are biodegradable raw materials that are physiologically tolerated [17]: triglycerides (i.e. tristearin), partial glycerides (i.e. Compritol), fatty acids (i.e. stearic acid), steroids (i.e. cholesterol) or waxes (i.e. cetyl palmitate) [18].

The formulation methods are also diverse. Emulsion formation and solvent evaporation method has been widely used for particle formation, although other methods like high pressure homogenization [18], solvent diffusion methods in aqueous solutions [19] or hot emulsion methods [18,20] have also been employed. Drawbacks associated to this kind of formulations, like limited drug loading capacity, adjustment of drug release profile and potential drug expulsion during storage, have been reported [21]. Besides, drug loading capacity is limited by the solubility of the drug in the lipid melt, the structure of the lipid matrix and the polymorphic state of the lipid matrix.

Comparing with the previously mentioned liposomes, the main improvement of the lipid nanoparticles is their physical and chemical long-term stability up to 12–24 months [13], even though an increase in particle size has been reported in a lesser time [22]. As a feasible solution for this setback, the freeze-drying process has shown to increase physicochemical stability of lipid particles over large periods of time [23].

Taking into account this information, the aim of this study was to develop a new formulation which would provide a controlled release for the antitumor lipid edelfosine, in order to improve its therapeutic activity.

## 2. Materials and methods

### 2.1. Materials

Edelfosine was from INKEYSA (Barcelona, Spain). Compritol® 888 ATO was a gift of Gattefossé (Cedex, France). Stearic acid and Tween® 80 were purchased from Roig Farma (Barcelona, Spain). Poly (vinyl alcohol) 88% hydrolyzed (MW: ~125,000) and Phosphate Buffer Saline (PBS) were provided by Sigma-Aldrich (Barcelona, Spain). Chloroform and ethyl acetate were obtained from Panreac Química S.A. (Barcelona, Spain). All solvents employed for the chromatographic analysis were of analytical grade. Formic acid 99% for mass spectroscopy was purchased from Fluka (Barcelona, Spain) and methanol was obtained from Merck (Barcelona, Spain). All other chemicals were of reagent grade and used without further purification.

Amicon Ultra-15 centrifugal filter devices were purchased from Millipore (Cork, Ireland).

### 2.2. Preparation of lipid nanoparticles

Lipid nanoparticles were prepared by the emulsification/solvent evaporation method. Since edelfosine is an amphiphilic molecule, simple and multiple emulsions were tested. For the simple emulsion solvent evaporation method, edelfosine and the lipid (100 mg of either Compritol® or stearic acid) were dissolved in 2 mL of chloroform. This solution was emulsified with 10 mL of a 0.5% or 1% Tween 80 solution by ultrasonication using a Microson™ ultrasonic cell disruptor (NY, USA). The O/W emulsion formed was magnetically stirred for 45 min and subjected to low vacuum rotary evaporation for the complete elimination of the organic solvent. Particles were centrifuged at 4500g for 40 min using an Amicon Ultra-15 filter device and washed twice with distilled water. The obtained particular suspension was fast frozen under  $-80^{\circ}\text{C}$  for at least 3 h and freeze-dried in order to store it at  $4^{\circ}\text{C}$ . For the double emulsion (W/O/W), edelfosine was dissolved in 100  $\mu\text{L}$  of a 1% Tween 80 solution and emulsified with 2 mL of ethyl acetate. This first W/O emulsion was then emulsified with 10 mL of a 1% Tween 80 solution. Following steps were the same to the ones of the simple emulsion solvent evaporation method.

### 2.3. Encapsulation efficiency

Edelfosine was extracted by dissolving 10 mg of nanoparticles in 1 mL of chloroform and then mixed with 3 mL of ultrapure water. The mixture was vortexed for 1 min and then centrifuged at 9500g for 10 min. The supernatant was analysed by a HPLC-MS method, which is a slight modification of a previously developed method [24]. The apparatus used for the HPLC analysis was a Model 1100 series LC coupled with an atmospheric pressure (AP)-electrospray ionization (ESI) mass spectrometer (HP 1100 with MSD VL, Waldbronn, Germany). Data acquisition and analysis were performed with a Hewlett-Packard computer using the ChemStation G2171 AA programme. Separation was carried out at  $50^{\circ}\text{C}$  on a reversed-phase, 150 mm  $\times$  3 mm column packed with C18, 5  $\mu\text{m}$  silica reversed-phase particles (Gemini®) obtained from Phenomenex® (Torrance, CA, USA). This column was preceded by a reversed-phase, C18, 5  $\mu\text{m}$  guard column (SecurityGuard®, 20 mm  $\times$  4 mm, Phenomenex®, Torrance, CA, USA). The mobile phase was a mixture of methanol–1% formic acid (95:5, v/v). Separation was achieved by isocratic solvent elution at a flow rate of 0.5 mL/min. The mass spectrometer was operated in the positive ESI mode. The detection of edelfosine was performed by selected ionization monitoring (SIM) mode. The mass spectrometer was programmed to monitor the ion of edelfosine at  $m/z$  524.40. Typical retention time was 3.65 min.

## 2.4. Nanoparticle characterization

### 2.4.1. Particle size, size distribution and zeta potential

Particle size and distribution of the nanoparticles were measured by photon correlation spectroscopy (PCS) using a Zetasizer Nano (Malvern Instruments, UK). Each sample was diluted 30-fold in distilled water until the appropriate concentration of particles was achieved to avoid multiscattering events. The obtained homogeneous suspension was examined to determine the volume mean diameter, size distribution and polydispersity and repeated three times for each sample. The data are expressed as a mean values  $\pm$  standard deviation.

Similarly, the zeta potential was measured using the same equipment described previously with a combination of laser Doppler velocimetry. Samples were diluted with distilled water and each experiment was repeated three times.

### 2.4.2. Morphology

Atomic force microscopy (Cervantes AFM System, Nanotec Electrónica, S.L., Spain) was employed to determine the shape and surface morphology of the nanoparticles. AFM was conducted with Nanoscope IIa IIIa in the tapping mode. The nanoparticle sample was mounted on a metal stab and scanned by the AFM maintained in a constant temperature and vibration time environment.

### 2.4.3. Thermal analysis of freeze-dried lipid nanoparticles

The thermal characteristics of selected batches of nanoparticles were determined by differential scanning calorimetry thermal analysis using a 2920 DSC (Universal V3.6C TA Instruments, USA). The scan rate was 10 °C/min in the temperature range from  $-10$  °C to 275 °C and a  $N_2$  flow rate of 20 L/min. An empty pan was used as reference standard. Indium (purity  $\geq 99.95\%$ , Fluka, Switzerland) was employed to check the calibration of the calorimetric system.

### 2.4.4. X-ray studies of freeze-dried lipid nanoparticles

X-ray diffraction measurements were performed in order to clearly elucidate the solid state of both lipids and drug in lipid nanoparticles, using a Bruker D8 Advance X-ray diffractometer (Bruker Biosciences Española, S.A., Spain). The X-ray diffractogram was scanned with the diffraction angle increasing from 2° to 40°,  $2\theta$  angle, with a step angle of 0.02° and a count time of 1 s at a constant temperature of 25 °C.

## 2.5. *In vitro* release studies

The release rate of edelfosine from lipid nanoparticles was measured in PBS medium (pH 7.4). Briefly, 5 mg of nanoparticles was dispersed in 1 ml of buffer solution and maintained at 37 °C under stirring (260 rpm). At appropriate time intervals, samples were centrifuged (23,500g, 10 min), supernatants were filtered with a 0.45  $\mu$ m pore

diameter filter and kept at  $-20$  °C until further HPLC-MS analysis was conducted as previously described. Three samples were employed for each time and the study was performed in triplicate.

The mean *in vitro* dissolution time (MDT), a model-independent *in vitro* parameter that shows the meantime for edelfosine to release from the lipid nanoparticles under *in vitro* release conditions, was calculated according to the equation:

$$MDT = \frac{ABC_{in\ vitro}}{M_{\infty}} \quad (1)$$

where  $ABC_{in\ vitro}$  is the area between the release curve and its asymptote, calculated by the trapezoidal rule from time zero to the last measured time point, and  $M_{\infty}$  is the total amount of released drug at this time point. The release rate constant ( $k_d$ ) was calculated by the expression  $k_d = 1/MDT$ .

## 3. Results and discussion

### 3.1. Particle size, size distribution and zeta potential

Structurally, edelfosine has a structure of an amphiphile, with a part of the molecule exhibiting hydrophobicity and another part exhibiting hydrophilicity, like a surface-active agent (Fig. 1).

Edelfosine-loaded lipid nanoparticles were obtained by either simple or multiple emulsion solvent evaporation method, and freeze-dried. These nanoparticles were then characterized to assess the effect of the different lipids and surfactant concentrations on mean particle size, size distribution and surface charge.

Using lipids as matrices for the particles, different characteristics can be obtained by optimizing the formulation parameters such as type of lipids, surfactants, organic solvents and emulsifying procedure chosen [18]. The presence of a non-ionic surfactant is important to reduce the dynamic interfacial tension and to stabilize the nanosuspension. The surfactant is adsorbed on the nanoparticle surface, increasing the steric repulsion between particles. In this study, Tween® 80 was tested at two different concentrations (w/v), being sufficient to obtain small lipid nanoparticles and permitting the removal of its excess by centrifugation and washing.

The average size and polydispersity indices of lipid nanoparticles formulated with different lipids are reported

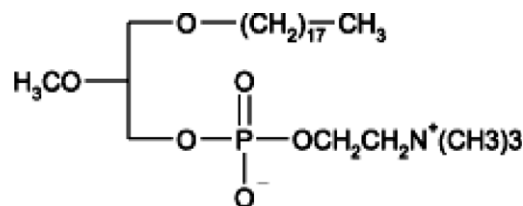


Fig. 1. Chemical structure of edelfosine.

in Table 1. All data are expressed as mean values  $\pm$  standard deviation. For all lipids, it was possible to obtain sub-micron sized lipid nanoparticles with two different concentrations of Tween<sup>®</sup> 80. In fact, all edelfosine loaded formulations showed a mean diameter in the range of 300–600 nm. There was a decrease in size of particles when formulated with edelfosine (data not shown), probably due to the effect of edelfosine as a surfactant agent. Smallest particles were obtained using stearic acid, chloroform and an aqueous solution of Tween<sup>®</sup> 80 at a concentration of 1%. The polydispersity index (PDI) value was in the range of 0.2–0.6 for all lipid nanoparticles investigated.

Zeta potential can make a prediction about the stability of colloid dispersions. A high zeta potential ( $>30$  mV) can provide an electric repulsion to avoid the aggregation of particles [25]. The incorporation of edelfosine into lipid nanoparticles had no significant influence on the zeta potentials of particles, which was negative in all cases. However, as the concentration of surfactant was increased in the formulation the zeta potential was found to be more negative (Table 1). This could be due to the presence of oleic acid traces (in Tween) on the particle surface, forming a denser surfactant film, thus eliciting an increased electrophoretic mobility.

### 3.2. Drug entrapment efficiency and loading capacity

Over the past few years many different drugs had been successfully incorporated in lipid nano- or microparticles [20,26–28]. Relatively high drug encapsulation efficiency for hydrophobic drugs was one of the major advantages of lipid nanoparticles [20]. It is also known that the lipid crystalline structure related to the chemical nature of the lipid is a key factor to determine whether a drug will be expelled or firmly incorporated into the carrier systems. In the nanoparticle structure, the lipid forming highly crystalline state with a perfect lattice would lead to drug expulsion. On the other hand, imperfections (lattice defects) of the lipid structure could offer space to accommodate the drugs [29]. As a result, the structure of less ordered arrangement in the nanoparticles would be beneficial to the drug loading capacity like the samples in this study.

From the results listed in Table 2, it can be observed that the entrapment efficiency of edelfosine in the lipid nanoparticles prepared by the simple emulsion solvent evaporation method ranged from about 4 to 10% for

Table 2

Encapsulation efficiency (EE) of the different nanoparticles prepared either with methylene chloride (MC) or trichloromethane (TCM)

| Lipid                          | Solvent | Stabilizing agent | %EE   |
|--------------------------------|---------|-------------------|-------|
| Stearic acid                   | MC      | Tween 80 0.5%     | 5.10  |
|                                |         | Tween 80 1%       | 4.00  |
|                                | TCM     | Tween 80 0.5%     | 9.20  |
|                                |         | Tween 80 1%       | 6.40  |
| Compritol <sup>®</sup> 888 ATO | TCM     | Tween 80 1%       | 84.35 |

stearic acid nanoparticles. On the other hand, nanoparticles formulated using Compritol<sup>®</sup> encapsulated more than 80% of the drug (Table 2). This high encapsulation efficiency in comparison to the stearic acid nanoparticles is likely to be due to the partially amorphous state of the Compritol<sup>®</sup> in the formulation, which allows more edelfosine to be incorporated among lipid chains. It can also be observed that the emulsifier concentrations investigated in this study (0.5% and 1% Tween 80) do not affect the encapsulation efficiency.

On the other hand, lipid nanoparticles prepared by the multiple emulsion solvent evaporation method showed very low encapsulation efficiency, less than 1% (data not shown).

### 3.3. Morphology

In order to investigate the shape and surface morphology of the Compritol<sup>®</sup> nanoparticles, atomic force microscopy was employed. The AFM images reveal the fine structure of the Compritol<sup>®</sup> lipid nanoparticle surface (Fig. 2A). They give clear 3D morphological images of spherical nanoparticles of sub-400 nm diameter and they also confirm that there was no aggregation or adhesion among the nanoparticles (Fig. 2C). Furthermore, the surface morphology of the nanoparticles could be seen closely from the AFM images. It was noticeable from the zoom-in picture (Fig. 2B) the smooth surface morphology of the nanoparticles.

### 3.4. DSC and X-ray diffractometry assays

Lipid nanoparticles were analysed by DSC and X-ray diffractometry to investigate the crystal pattern of both edelfosine and lipids, because this aspect could influence the *in vitro* and *in vivo* release of the drug from the systems.

Table 1

Average size, polydispersity index (PDI) and zeta potential of edelfosine loaded lipid nanoparticles ( $n = 13$ ) prepared either with methylene chloride (MC) or trichloromethane (TCM)

| Lipid                          | Solvent | Stabilizing agent | Size (nm)       | PDI              | ζ Potential (mV) |
|--------------------------------|---------|-------------------|-----------------|------------------|------------------|
| Stearic acid                   | MC      | 0.5% Tween 80     | 480 $\pm$ 10.79 | 0.204 $\pm$ 0.01 | −32.75           |
|                                |         | 1% Tween 80       | 611 $\pm$ 5.29  | 0.626 $\pm$ 0.13 | −35.15           |
|                                | TCM     | 0.5% Tween 80     | 415 $\pm$ 30.09 | 0.451 $\pm$ 0.09 | −29.33           |
|                                |         | 1% Tween 80       | 312 $\pm$ 7.51  | 0.225 $\pm$ 0.04 | −32.4            |
| Compritol <sup>®</sup> 888 ATO | TCM     | 1% Tween 80       | 372 $\pm$ 18.84 | 0.354 $\pm$ 0.06 | −32.3            |



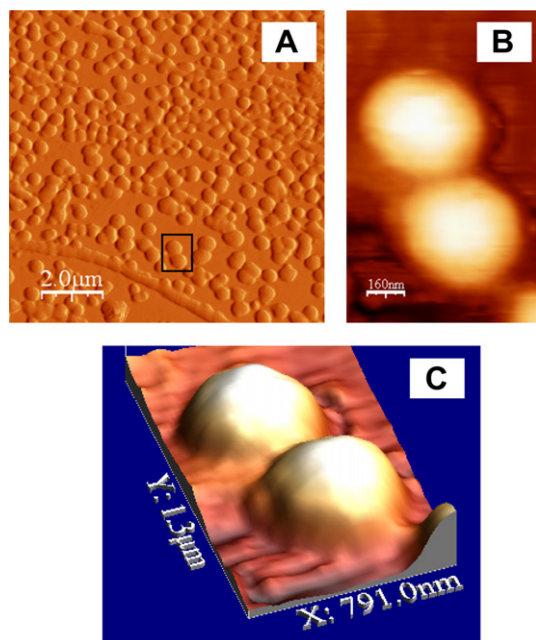


Fig. 2. Atomic force microscopy images of freeze-dried Compritol® lipid nanoparticles: multi-particles (a); zoom-in of the selected area of (A) (B); 3D morphological image (C).

To probe this effect, analysis was performed on the following samples: edelfosine; Compritol® 888 ATO; stearic acid; edelfosine loaded stearic acid nanoparticles; edelfosine loaded Compritol® nanoparticles; unloaded stearic acid nanoparticles; unloaded Compritol® nanoparticles.

Fig. 3 depicts the DSC thermograms of edelfosine loaded and unloaded lyophilised nanoparticles. As Compritol® is not composed of pure triacylglycerols, the observed melting peak at 72.43 °C might be due to a mixture of metastable polymorphic  $\beta$  and  $\beta'$  forms. The heating run showed the just mentioned melting event at 72.43 °C and a relatively small endothermic shoulder at around 51 °C. This small shoulder corresponds to the melting of a very unstable modification of Compritol®, which is the  $\alpha$  modification [30], that clearly disappears after the treatment with organic solvents for the nanoparticle preparation. DSC analysis of edelfosine-loaded lipid nanoparticles showed that the drug melting peak at 223 °C is present neither in the stearic acid lipid nanoparticles nor in the Compritol® lipid nanoparticles whereas for the pure drug, the melting peak occurs before its decomposition. This thermal behaviour may be ascribed to the presence of edelfosine in an amorphous form or molecularly dispersed, but it may also be related to a possible solubilisation of the drug in the molten lipid when the DSC assay was performed. Besides, X-ray diffraction studies support this theory showing a partial crystalline state of the drug. This effect on the crystalline habit of edelfosine may be related to the preparative method of the lipid nanoparticles, in which edelfosine may be turned from a crystalline state to an amorphous one by the use of organic solvents like chloroform or methylene chloride.

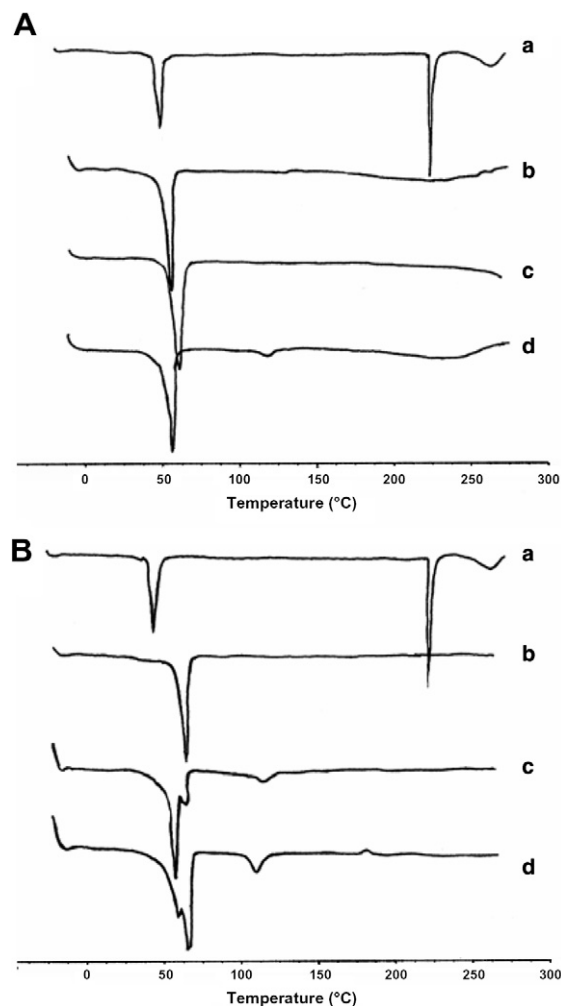


Fig. 3. DSC thermograms of: (a) edelfosine, (b) stearic acid, (c) unloaded stearic acid lipid nanoparticles and (d) edelfosine-loaded stearic acid lipid nanoparticles (A); (a) edelfosine, (b) Compritol®, (c) unloaded Compritol® lipid nanoparticles and (d) edelfosine-loaded Compritol® lipid nanoparticles (B).

Thermal behaviour of lipids can also explain the different encapsulation efficiency of edelfosine. Unloaded stearic acid nanoparticles showed the melting peak of the stearic acid at 59 °C, indicating its presence in crystalline state, thus letting less amount of drug to be incorporated among its lipidic chains. On the other hand, Compritol® nanoparticles seem to lose part of their crystalline state transforming from a mixture of  $\beta$  and  $\beta'$  polymorphs to the most stable  $\beta$  polymorph, permitting edelfosine to fit in the molecular gaps. These findings were confirmed by X-ray diffractometry assays. Unloaded stearic acid nanoparticles (Fig. 4A) show two sharp peaks corresponding to those of the stearic acid, whereas the diffraction pattern of bulk Compritol® (Fig. 4B) showed two main typical signals at 21.5 ( $2\theta$ ) and 23.5 ( $2\theta$ ) that are significantly modified when formulated into nanoparticles. Besides, when Compritol® nanoparticles are formulated, another signal arises at 19.4 ( $2\theta$ ) (Fig. 4B) which corresponds to the most stable polymorphic form of triacylglycerols  $\beta$  [30]. These results might indicate that the final formulation is composed of

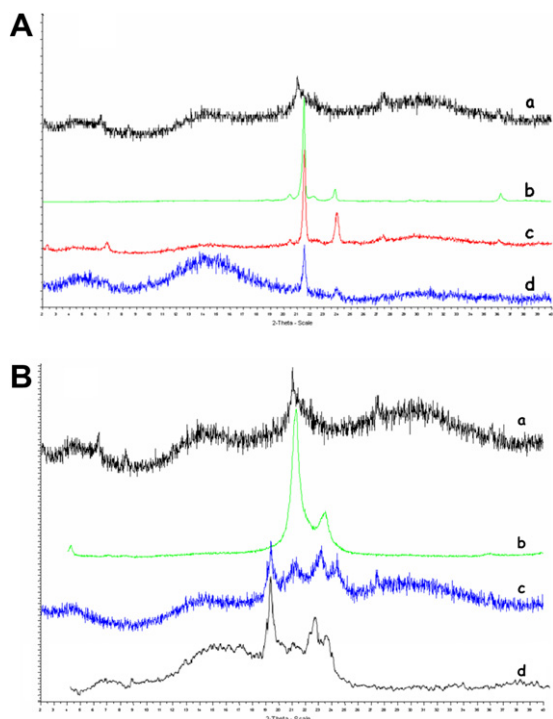


Fig. 4. X-ray diffractograms of: (a) edelfosine, (b) stearic acid, (c) unloaded stearic acid lipid nanoparticles and (d) edelfosine-loaded stearic acid lipid nanoparticles (A); (a) edelfosine, (b) Compritol®, (c) edelfosine-loaded Compritol® lipid nanoparticles and (d) unloaded Compritol® lipid nanoparticles (B).

the most stable polymorphic state of Compritol®. Comparing these results with edelfosine loaded lipid nanoparticles, some crystalline drug signal could still be detected, indicating a possible coexistence of edelfosine in both crystalline and amorphous states, being this last one the predominant. As a result, edelfosine would enrich the particle surface when formulated with stearic acid, whereas it would be incorporated among the lipid chains of Compritol®.

### 3.5. *In vitro* release studies

The amount of edelfosine released from lipid nanoparticles was determined by an *in vitro* release assay, in an effort to assess whether edelfosine-incorporating lipid nanoparticles might be useful as a sustained-release dosage form.

Fig. 5 displays the release profiles for nanoparticles fabricated with stearic acid or Compritol® using 1% Tween 80 as emulsifier. When edelfosine was incorporated in stearic acid nanoparticles, a 63% burst release of the drug was observed within 20 min (Fig. 5). Conversely, the initial release burst for nanoparticles prepared using Compritol® was less than 40% within the first 20 min. The reason for the high initial release of edelfosine from the stearic acid nanoparticles could be the diffusion release of edelfosine distributed near the surface and in the outer portion of the nanoparticles [12]. These results were in accordance with the observations made by DSC and X-ray diffractometry.

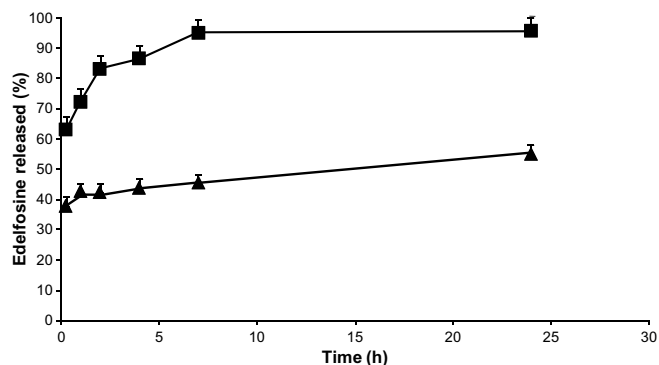


Fig. 5. *In vitro* release profiles of edelfosine from stearic acid lipid nanoparticles (■) and Compritol® 888 ATO nanoparticles (▲).

Afterwards, the release rate slowed for both formulations, reaching 55% after 24 h for nanoparticles prepared with Compritol®, and 98% for the stearic acid nanoparticles.

The release of a drug from the dosage form implies a crucial step, which is the dissolution of the drug. This process is ruled by a release rate constant ( $k_d$ ) that can be easily estimated and it is different depending, among other factors, on the composition of the particle. In our study, this constant was estimated for the release of edelfosine from lipid nanoparticles formulated either with stearic acid or Compritol®.

Results showed that there is a different release profile depending on the lipid. Stearic acid presents a higher release rate constant ( $k_d = 0.208$ ) than Compritol® ( $k_d = 0.178$ ), indicative of a faster release. Besides, there seems to be no influence of the amounts of surfactant employed in the release kinetics of the drug, since the release rate constant from nanoparticles prepared with different surfactant concentrations (0.5% or 1% Tween 80) was equivalent.

Nevertheless, the *in vitro* release rates cannot be directly extrapolated to predict behaviour of these systems in biological environments. The differences between *in vitro* and *in vivo* degradation of the nanoparticles can be ascribed to the presence of enzymes [31] and the prolonged release of the drug from the nanoparticulate systems has to be quantified in an *in vivo* animal model.

## 4. Conclusions

The present research paper proposed a novel formulation for edelfosine by using lipid nanoparticles. It can be concluded that Compritol® presents advantages as a matrix material for the manufacture of the nanoparticles and the controlled release of edelfosine.

Current studies are aimed at evaluating the *in vitro* (in cell lines) and *in vivo* efficacy of these newly developed formulations.

## Acknowledgements

This work was supported by “Fundación Caja Navarra” and by Ministerio de Educación y Ciencia (SAF2007-

61261). The authors are grateful to Nanotec Electrónica S.L. and Dr. Blanca Galar for her assistance in X-ray diffraction studies. The first author acknowledges a fellowship from the Department of Education of the Basque Government.

## References

- [1] C. Gajate, F. Mollinedo, Biological activities, mechanisms of action and biomedical prospect of the antitumor ether phospholipid ET-18-OCH<sub>3</sub> (edelfosine), a proapoptotic agent in tumor cells, *Curr. Drug Metab.* 3 (5) (2002) 491–525.
- [2] W.E. Berdel, U. Fink, J. Rastetter, Clinical phase I pilot study of the alkyl lysophospholipid derivative ET-18-OCH<sub>3</sub>, *Lipids* 22 (11) (1987) 967–969.
- [3] F. Mollinedo et al., Selective induction of apoptosis in cancer cells by the ether lipid ET-18-OCH<sub>3</sub> (Edelfosine): molecular structure requirements, cellular uptake, and protection by Bcl-2 and Bcl-X(L), *Cancer Res.* 57 (7) (1997) 1320–1328.
- [4] C. Gajate, F. Mollinedo, Edelfosine and perifosine induce selective apoptosis in multiple myeloma by recruitment of death receptors and downstream signaling molecules into lipid rafts, *Blood* 109 (2) (2007) 711–719.
- [5] F. Mollinedo, Antitumour ether lipids: proapoptotic agents with multiple therapeutic indications, *Expert Opin. Therap. Patents* 17 (4) (2007) 385–405.
- [6] S. Azzouz et al., Leishmanicidal activity of edelfosine, miltefosine and ilmofosine, *Basic Clin. Pharmacol. Toxicol.* 96 (1) (2005) 60–65.
- [7] K.P. Boggs, C.O. Rock, S. Jackowski, Lysophosphatidylcholine and 1-*O*-octadecyl-2-*O*-methyl-rac-glycero-3-phosphocholine inhibit the CDP-choline pathway of phosphatidylcholine synthesis at the CTP:phosphocholine cytidyltransferase step, *J. Biol. Chem.* 270 (13) (1995) 7757–7764.
- [8] W.R. Vogler et al., The anticancer drug edelfosine is a potent inhibitor of neovascularization in vivo, *Cancer Invest.* 16 (8) (1998) 549–553.
- [9] B. Zheng et al., Inhibition of protein kinase C, (sodium plus potassium)-activated adenosine triphosphatase, and sodium pump by synthetic phospholipid analogues, *Cancer Res.* 50 (10) (1990) 3025–3031.
- [10] I. Ahmad et al., Enhanced therapeutic effects of liposome-associated 1-*O*-octadecyl-2-*O*-methyl-sn-glycero-3-phosphocholine, *Cancer Res.* 57 (10) (1997) 1915–1921.
- [11] R. Bhamra et al., Activity, pharmacokinetics and tissue distribution of TLC ELL-12 (liposomal antitumor ether lipid) in rats with transplantable, s.c. methylnitrosourea-induced tumors, *Anticancer Drugs* 14 (6) (2003) 481–486.
- [12] A. zur Muhlen, C. Schwarz, W. Mehnert, Solid lipid nanoparticles (SLN) for controlled drug delivery – drug release and release mechanism, *Eur. J. Pharm. Biopharm.* 45 (2) (1998) 149–155.
- [13] B. Siekmann, K. Westesen, Sub-micron sized parenteral carrier systems based on solid lipids, *Pharm. Pharmacol. Lett.* 1 (1992) 123.
- [14] C. Schwarz, W. Mehnert, Solid lipid nanoparticles (SLN) for controlled drug delivery. II. Drug incorporation and physicochemical characterization, *J. Microencapsul.* 16 (2) (1999) 205–213.
- [15] T. de Vringer, H.A. de Ronde, Preparation and structure of a water-in-oil cream containing lipid nanoparticles, *J. Pharm. Sci.* 84 (4) (1995) 466–472.
- [16] A.J. Almeida, S. Runge, R.H. Muller, Peptide-loaded solid lipid nanoparticles (SLN): influence of production parameters, *Int. J. Pharm.* 149 (2) (1997) 255–265.
- [17] S.A. Wissing, O. Kayser, R.H. Muller, Solid lipid nanoparticles for parenteral drug delivery, *Adv. Drug Deliv. Rev.* 56 (9) (2004) 1257–1272.
- [18] W. Mehnert, K. Mader, Solid lipid nanoparticles: production, characterization and applications, *Adv. Drug Deliv. Rev.* 47 (2–3) (2001) 165–196.
- [19] F.Q. Hu et al., Preparation and characterization of stearic acid nanostructured lipid carriers by solvent diffusion method in an aqueous system, *Colloids Surf. B Biointerfaces* 45 (3–4) (2005) 167–173.
- [20] S. Jaspert et al., Solid lipid microparticles as a sustained release system for pulmonary drug delivery, *Eur. J. Pharm. Biopharm.* 65 (1) (2007) 47–56.
- [21] R.H. Muller, M. Radtke, S.A. Wissing, Nanostructured lipid matrices for improved microencapsulation of drugs, *Int. J. Pharm.* 242 (1–2) (2002) 121–128.
- [22] C. Freitas, R.H. Muller, Effect of light and temperature on zeta potential and physical stability in solid lipid nanoparticles (SLN) dispersion, *Int. J. Pharm.* 168 (1998) 221–229.
- [23] R. Cavalli et al., Sterilization and freeze-drying of drug-free and drug-loaded solid lipid nanoparticles, *Int. J. Pharm.* 148 (1997) 47–54.
- [24] M.J. Blanco-Prieto, M.A. Campanero, F. Mollinedo, Quantitative determination of the antitumor alkyl ether phospholipid edelfosine by reversed-phase liquid chromatography-electrospray mass spectrometry: application to cell uptake studies and characterization of drug delivery systems, *J. Chromatogr. B Anal. Technol. Biomed. Life Sci.* 810 (1) (2004) 85–92.
- [25] M.Y. Levy et al., Characterization of diazepam submicron emulsion interface: role of oleic acid, *J. Microencapsul.* 11 (1) (1994) 79–92.
- [26] H. Chen et al., Podophyllotoxin-loaded solid lipid nanoparticles for epidermal targeting, *J. Control Release* 110 (2) (2006) 296–306.
- [27] F.Q. Hu et al., Preparation of solid lipid nanoparticles with clobetasol propionate by a novel solvent diffusion method in aqueous system and physicochemical characterization, *Int. J. Pharm.* 239 (1–2) (2002) 121–128.
- [28] M.K. Lee, S.J. Lim, C.K. Kim, Preparation, characterization and in vitro cytotoxicity of paclitaxel-loaded sterically stabilized solid lipid nanoparticles, *Biomaterials* 28 (12) (2007) 2137–2146.
- [29] D. Hou et al., The production and characteristics of solid lipid nanoparticles (SLNs), *Biomaterials* 24 (10) (2003) 1781–1785.
- [30] E.B. Souto, W. Mehnert, R.H. Muller, Polymorphic behaviour of Compritol 888 ATO as bulk lipid and as SLN and NLC, *J. Microencapsul.* 23 (4) (2006) 417–433.
- [31] C. Olbrich, R.H. Muller, Enzymatic degradation of SLN-effect of surfactant and surfactant mixtures, *Int. J. Pharm.* 180 (1) (1999) 31–39.